Available online at www.sciencedirect.com
ScienceDirect
Trans. Nonferrous Met. Soc. China 21(2011) 725−731
Transactions of Nonferrous Metals Society of China
www.tnmsc.cn

Effects of Sr and Y on microstructure and corrosion resistance of AZ31 magnesium alloy

CHEN Gang[1, 2], PENG Xiao-dong[2, 3], FAN Pei-geng[1], XIE Wei-dong[2, 3], WEI Qun-yi[2], MA Hong[2], YANG Yan[2]

1. College of Metallurgy and Materials Engineering, Chongqing University of Science and Technology, Chongqing 401331, China;
2. College of Materials Science and Engineering, Chongqing University, Chongqing 400044, China;
3. National Engineering Research Center for Magnesium Alloy, Chongqing 400044, China

Received 25 September 2010; accepted 25 December 2010

Abstract: The effects of Sr and Y with different contents on the microstructure and corrosion resistance of AZ31 alloy were investigated. The results indicate that the addition of Sr can obviously reduce the grain size of AZ31 alloy and transform β-$Mg_{17}Al_{12}$ phase from continuous network to scattered form. Simultaneously, Al_4Sr phase distributed along the boundaries of grains is formed in AZ31-Sr magnesium alloys. The addition of Sr is not as effective as the simultaneous addition of Sr+Y for the refinement of grains, and Al_2Y and Al_3Y phases are distributed both in intracrystalline and along grain boundaries. The corrosion resistance is improved slightly in AZ31 alloy with simultaneous addition of 0.5%Sr+Y. Due to its smallest corrosion current density and corrosion rate, the corrosion resistance of AZ31-0.5%Sr-1.5%Y magnesium alloy is proved the best.

Key words: AZ31 magnesium alloy; strontium; yttrium; corrosion resistance

1 Introduction

Magnesium alloy is the lightest structural metal and has the highest specific strength in the commonly used metallic materials, thus, it is very attractive for structural applications, particularly in the automobile industry[1−4]. But its applications are rather limited due to the relatively low absolute strength and ductility values resulted from the symmetric hexagonal close-packed crystal structure and poor corrosion resistance[5−7], Therefore, it is necessary to improve the mechanical properties and corrosion resistance of magnesium and its alloys.

Grain refinement is an important method to improve the mechanical properties and workability of both cast and wrought magnesium alloys. It was reported that the addition of Ca, Sr and rare earth(RE) elements is effective to improve the performance of magnesium alloy[8−10]. In recent years, some technologies have been developed to improve the corrosion resistance of magnesium alloy, such as coating technologies, surface treatment technologies and alloying technologies. But coating technologies and surface treatment technologies would cause many environmental problems. Therefore, alloying technology has been paid more attention to improve the corrosion resistance of magnesium and its alloys. RE elements have distinguished feature of corrosion resistance enhancement for magnesium alloys[11−15]. ZHANG et al[16] reported that the addition of Y to AZ91 alloy could refine the microstructure and improve the corrosion resistance. Nevertheless, there were few reports about the effects of Sr and Y on the corrosion resistance of AZ31 alloy. Meanwhile, the combinative role of Sr and Y on the microstructure and corrosion resistance of magnesium alloy has not been systematically investigated.

AZ31 Mg alloy is one of the popular wrought alloys which have received the most attention regarding to the structure-property correlation and formability. In this work, the influences of Sr and Y with different contents on the microstructure and corrosion resistance of AZ31 alloy are investigated. The aim of the present research is to develop an effective way to refine the microstructure and improve the corrosion resistance of AZ31 alloy.

Foundation item: Project (2007CB613702) supported by the National Basic Research Program of China; Project (2006AA4012) supported by the Research Program Foundation of CQ CSTC, China; Project (2008BB4323) supported by the Natural Science Foundation of CQ CSTC, China
Corresponding author: CHEN Gang; Tel:+86-23-65023707; E-mail:love.cg@163.com
DOI: 10.1016/S1003-6326(11)60772-3

2 Experimental

2.1 Material preparation

The AZ31 alloy was prepared from pure magnesium (99.99%), pure aluminum (99.95%) and pure zinc (99.99%). Sr and Y were added in the form of master alloys containing Mg-10%Sr and Mg-30%Y, respectively. The chemical composition of the experimental alloys is listed in Table 1.

Table 1 Chemical composition of alloys (mass fraction, %)

Alloy	Al	Zn	Sr	Y	Mg
AZ31	3	0.8	−	−	Bal.
AZ31-0.5%Sr	3	0.8	0.46	−	Bal.
AZ31-0.5%Sr-0.5%Y	3	0.8	0.48	0.47	Bal.
AZ31-0.5%Sr-1.0%Y	3	0.8	0.53	1.04	Bal.
AZ31-0.5%Sr-1.5%Y	3	0.8	0.54	1.53	Bal.
AZ31-0.5%Sr-2.0%Y	3	0.8	0.45	1.99	Bal.

Pure magnesium and pure aluminum were melted in a carbon steel crucible under a protective atmosphere of CO_2 and SF_6 gas mixture. When magnesium and aluminum were melted completely, pure zinc, Mg-10%Sr and Mg-30%Y (mass fraction) master alloys were added to the molten alloy at about 740 °C. Then, the smelting was held at 740 °C for 30 min with mechanical stirring to make sure that the added elements were dissolved homogeneously. Casting was conducted at about 720 °C.

The specimens for salt spray test and electrochemical measurement were cut from the mid portion of the alloy ingots individually, and the dimensions of specimen are 15 mm × 5 mm × 5 mm.

2.2 Salt spray test

The salt spray test was performed in the FQY025 salt spray cabinet at 35 °C for 48 h. The corrosive medium was 3.5% NaCl solution, and the pH value was 7.5.

The tested specimens were gently washed by water after the test, and dipped into the solution of 200 g/L CrO_3 and 10 g/L $AgNO_3$ for 7 min to remove the salt deposits from the surface, then washed by acetone and distilled water, and immediately dried and finally weighed.

2.3 Electrochemical measurements

The electrochemical measurements were conducted using CHI660 electrochemical workstation. The corrosive medium was 3.5% NaCl solution, and the three-electrode system was used with 232 model saturated calomel electrode as reference electrode, AZ31 alloy as working electrode and 213 model Pt electrode as auxiliary electrode.

When the open circuit potential (OCP) became stable after the specimens were immersed into the 3.5 % NaCl solution for about 100 s, the potentiodynamic polarizations scanning started to perform from 300 mV relative to OCP and stopped at a potential where the corresponding current density held a stationary value. The scanning rate was 0.5 mV/s.

2.4 SEM observation, EDS and XRD analyses

The microstructures and morphologies of the alloys were characterized using optical microscope (OM, XJP-6A), and scanning electron microscope (SEM, TESCAN VEGA 2) the coupled energy dispersive spectroscope (EDS, Genesis 7000 X) and X-ray diffraction analysis (XRD, D/MAX-IIIC X) were used to identify the composition of the alloys.

3 Results and discussion

3.1 As-cast microstructure of alloys

The as-cast AZ31 alloy consisted of α-Mg, eutectic magnesium phase and β phase ($Mg_{17}Al_{12}$) as shown in Figs.1(a) and 2(a).

β phase has two functions in corrosion. On one hand, it can accelerate the corrosion of magnesium alloy as a cathode for its higher corrosion potential than that of the surrounding bulk material α-Mg. On the other hand, it

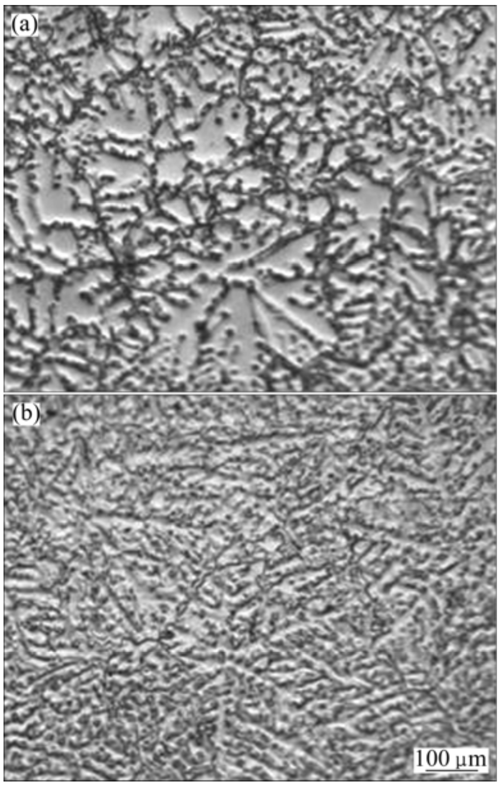

Fig.1 Optical microstructures of AZ31-xSr alloys: (a): x=0; (b) x=0.5%

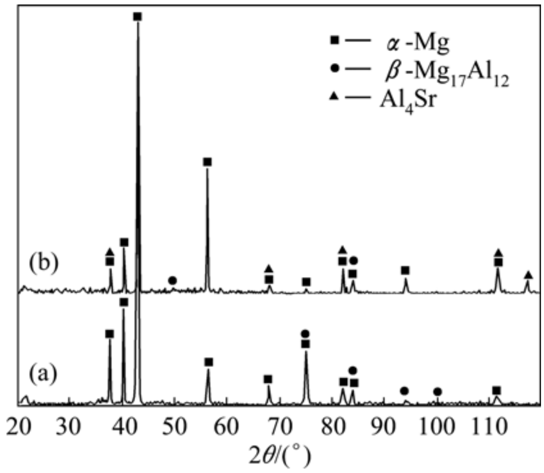

Fig.2 XRD patterns of AZ31 (a) and AZ31-0.5%Sr (b) magnesium alloys

can inhibit the corrosion of magnesium alloy as an impediment for a stable and allitic passivating film formed on its surface[11]. So the alloy with higher volume fraction and more continuous β phase shows better corrosion resistance.

Figure 2(b) shows the XRD pattern of AZ31 magnesium alloy with the addition of 0.5%Sr (mass fraction). It is clear that AZ31-0.5%Sr alloy consists of α-Mg, β-$Mg_{17}Al_{12}$ and Al_4Sr phases. The optical microstructure of AZ31-0.5%Sr is shown in Fig.1(b). It is observed that the grains of α-Mg are refined obviously, continuous distribution of β-phase turns into a network of discontinuous granular distribution, small dendrite structure is formed and small snow flake-like particles are dispersed on the grain boundaries.

The microstructures of as-cast AZ31 alloy containing 0.5%Sr and different content of Y are shown in Fig.3. It is shown that the grain refinement of AZ31 alloy by simultaneously adding 0.5%Sr+xY (mass fraction) is more obvious and the microstructure is more uniform than that by adding Sr alone. Black needle-like phase and granular particles appear along the grain boundaries simultaneously. When 0.5%Sr and 0.5%Y are added to AZ31 alloy, dendrites appear obviously in the microstructure. The black particles distribute between the secondary dendrites. When the Y content increases to 1.0%, equiaxed grains appear in the microstructure and small rod phase disperses in grain boundaries. When Y content is 1.5%, the grain size is the smallest and the distribution of rod-shaped grain boundaries and intracranial particles is more uniform. When Y content is 2.0%, the grains become coarse, the crystalline secondary phases within the clusters hold into groups, and the rod-shaped phase on the grain boundary links to network. EDS analysis suggests that the rod-like phase may be Al_4Sr phase. In addition, some massive particles are distributed on the grain boundaries as well as in the grain interior as shown in Figs.4(g) and (h). These massive particles may be $MgAl_4Y$[11].

The reason is due to two aspects. On one hand, the rare earth Y acts as heterogeneous nucleation. On the other hand, the solidification is limited by diffusion kinetics, which results in the enrichment of Y in the solid/liquid interface. An increment of constitutional supercooling leads to the change of crystal form, meanwhile, the rare-earth phase most distributing along the grain boundaries hinders the grains and $Mg_{17}Al_{12}$ phases growing up, which reduces the secondary dendrite arm of AZ31 magnesium alloy and turns the microstructure form of the alloys from typical dendrite to fine equiaxed.

Figure 4 shows the EDS spectra of the herring bone structure, particle phase and matrix phase of the AZ31-0.5%Sr-1.5%Y magnesium alloy. XRD analysis in Fig.5 suggests that the bone-like structure (as shown in Fig.4(a) point A) and particulate phase (as shown in Fig.4(a) point B) are Al_2Y and Al_3Y, respectively. According to the EDS analysis and XRD analysis, the phases composition of AZ31 magnesium alloy simultaneously added with 0.5%Sr +1.5%Y are α-Mg, β-$Mg_{17}Al_{12}$, Al_4Sr , Al_2Y and Al_3Y.

3.2 Analysis of salt spray test

The mass loss rate curve of AZ31-0.5%Sr-xY magnesium alloy immersed in 3.5% NaCl solution for 20 h is shown in Fig.6. The corrosion products were removed from the samples every 2 h for the solution continuously measurement.

It is seen that the corrosion rate decreases after simultaneously adding the Sr and Y to AZ31 magnesium alloy. It is indicated that Y can improve the corrosion resistance of AZ31 magnesium alloy greatly. The corrosion rate of AZ31-0.5%Sr-1.5%Y magnesium alloy was the minimum of 0.262 mg/(cm^2·h) and the corrosion resistance is the best.

The corrosion morphologies of the alloys after salt spray test in 3.5 % NaCl solution for 20 h are shown in Fig.7. It suggests that the corrosion of AZ31-0.5%Sr-0.5%Y, AZ31-0.5%Sr-1%Y and AZ31-0.5%Sr-2%Y alloys is much worse than that of AZ31-0.5%Sr-1.5%Y. Most of the corrosion products drop from the surface of AZ31-0.5%Sr-0.5%Y, AZ31-0.5%Sr-1%Y and AZ31-0.5%Sr-2%Y alloy specimens (shown in Figs.7(a), (b) and (d)). However, the specimen of AZ31-0.5%Sr-1.5%Y alloy is etched, as shown in Fig.7(c). Therefore,

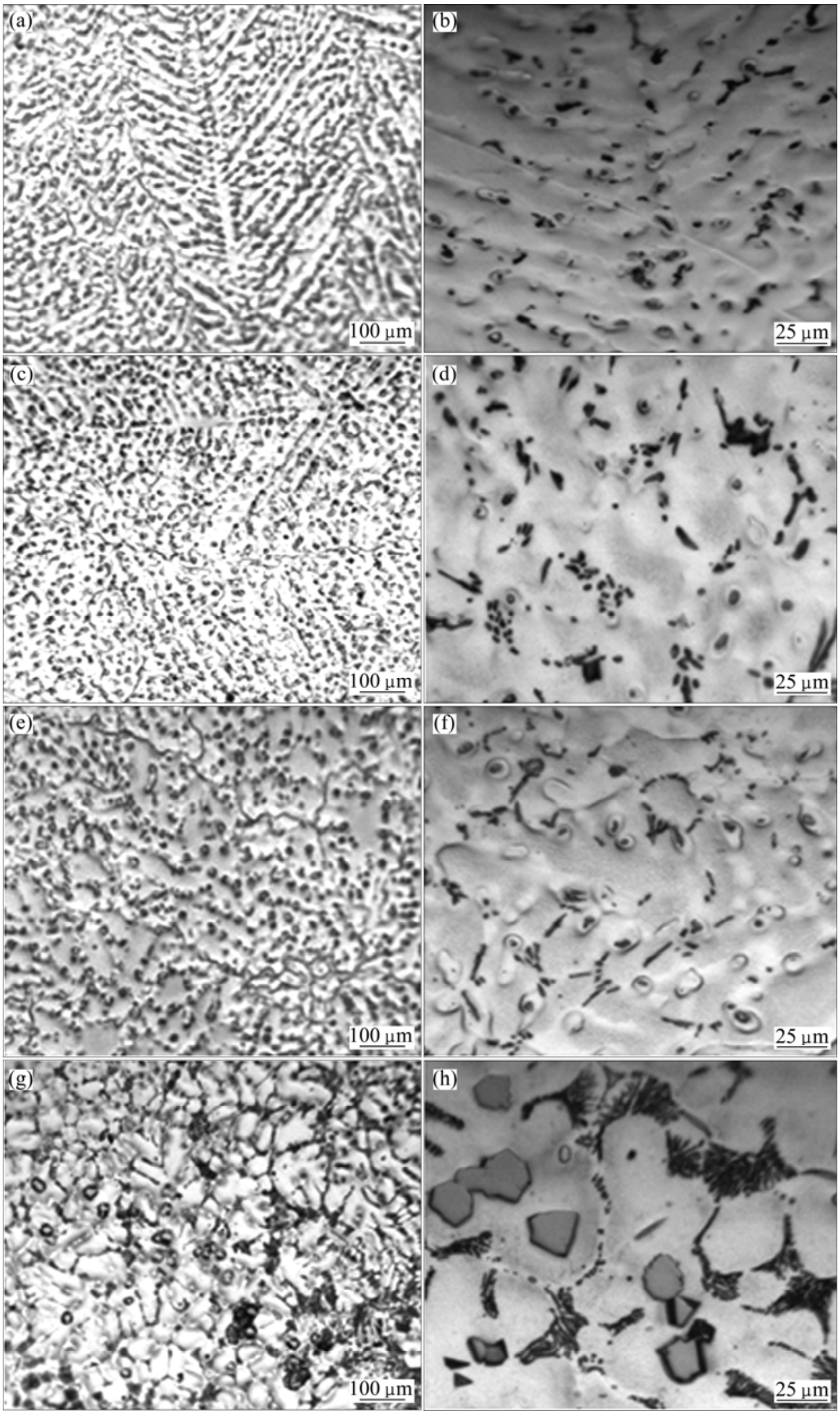

Fig.3 Optical microstructures of AZ31-0.5%Sr-xY magnesium alloys with different x values: (a), (b) 0.5%; (c), (d) 1.0%; (e), (f) 1.5%; (g), (h) 2.0%

AZ31-0.5%Sr-1.5%Y specimen is corroded slightly, and its surface is just of selective corrosion, which is consistent with the corrosion rate of the alloy.

3.3 Polarization curves

Figure 8 shows the potentiodynamic Tafel polarization curves of AZ31-0.5%Sr-xY alloy in 3.5%

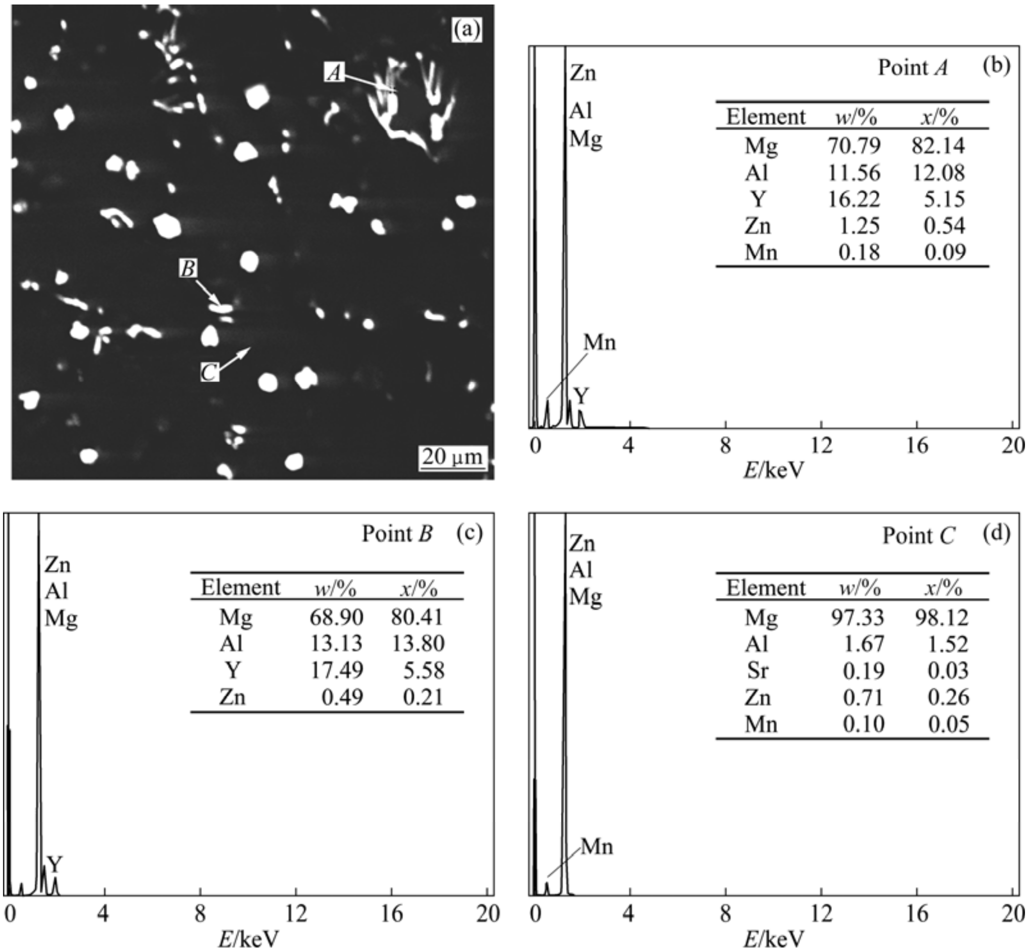

Fig.4 SEM morphology (a) and corresponding EDS analysis (b, c, d) of AZ31-0.5%Sr-1.5%Y magnesium alloy

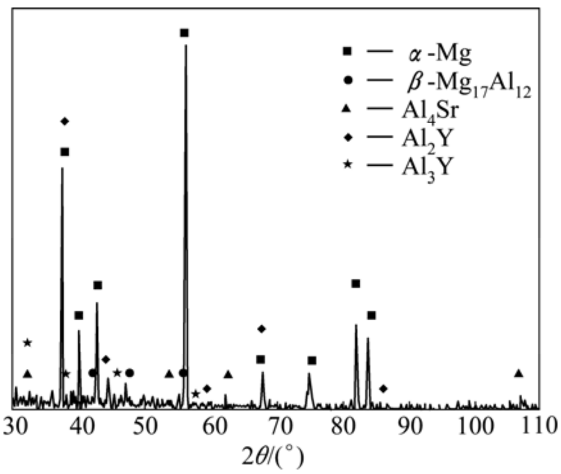

Fig.5 XRD pattern of AZ31-0.5%Sr-1.5%Y magnesium alloy

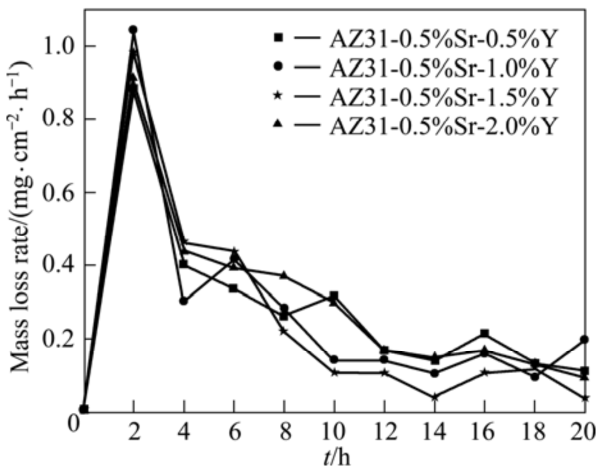

Fig.6 Mass loss rate curves of AZ31-0.5%Sr-*x*Y alloys after immersion in 3.5% NaCl solution for 20 h

NaCl solution. The current density decreases owing to the corrosion product formed before the cathodic corrosion reaction of hydrogen generates to protect the alloy. When the corrosion of the alloy occurs, the corrosion products are damaged and fall off, thus the current density rises sharply. Once the new corrosion products generate and protect the substrate well, the current of the alloy increases slowly and steadily, which is not obvious in the test pitting. With the simultaneous addition of Y and Sr, the corrosion potential of AZ31 alloy significantly negatively shifts and improves the corrosion resistance of AZ31 magnesium alloy. The results are listed in Table 2.

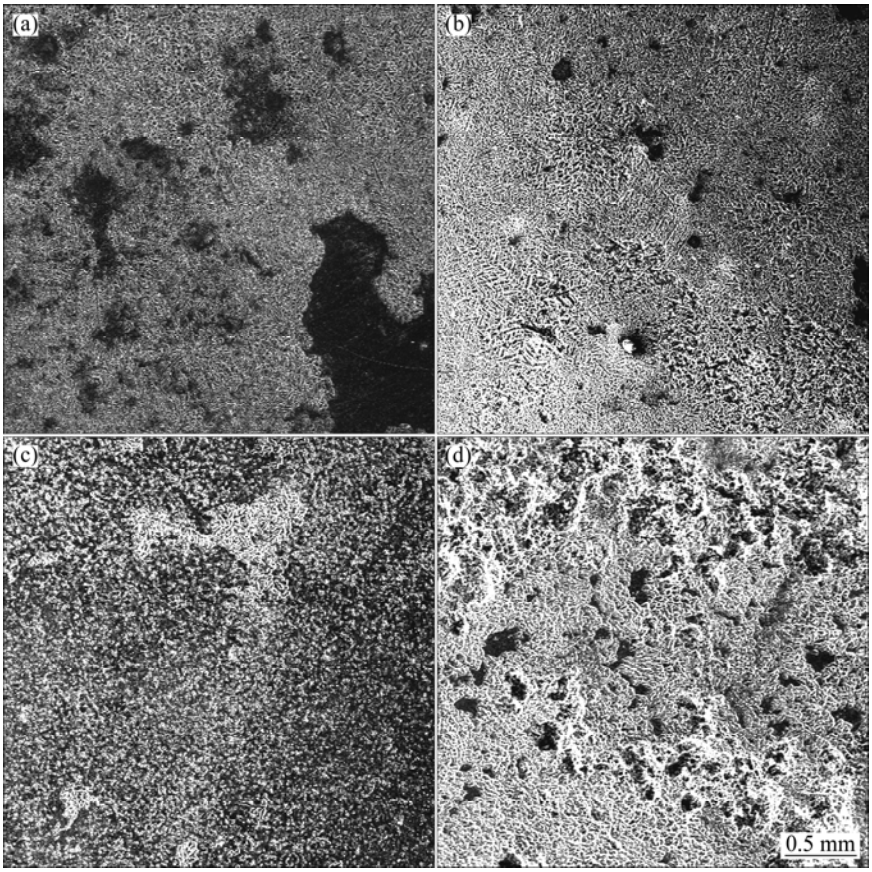

Fig.7 SEM images of corrosion surfaces of AZ31-0.5%Sr-xY magnesium alloys in 3.5% NaCl solution after 20 h immersion: (a) x=0.5%; (b) x=1%; (c) x=1.5%; (d) x=2%

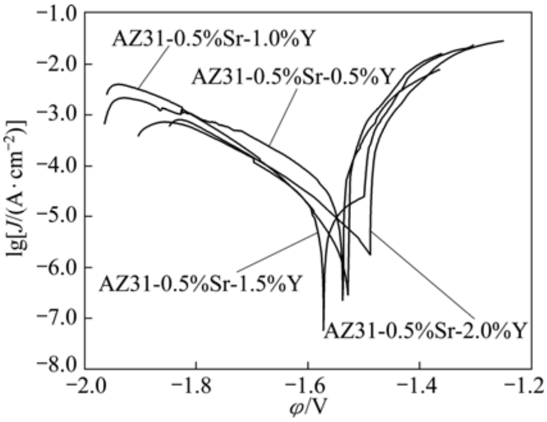

Fig.8 Tafel polarization curves of AZ31-0.5%Sr-xY magnesium alloys

Table 2 Tafel fitting results of polarization curves of AZ31-0.5%Sr-xY

Alloy	φ_{corr}/V	φ_{corr}/V	I_{corr}/A
AZ31	−1.567 6	−1.492	1.766×10^{-4}
AZ31-0.5%Sr-0.5%Y	−1.603 0	−1.502	4.732×10^{-5}
AZ31-0.5%Sr-1%Y	−1.659 1	−1.548	2.113×10^{-5}
AZ31-0.5%Sr-1.5%Y	−1.746 1	−1.605	1.836×10^{-6}
AZ31-0.5%Sr-2%Y	−1.662 3	−1.553	7.864×10^{-5}

From Table 2, it can be seen that the corrosion current I_{coor} of AZ31-0.5%Sr-1.5%Y magnesium alloy is the minimum, which decreases by almost two orders of magnitude and the corrosion resistance of AZ31-0.5%Sr-1.5%Y magnesium alloy is better than that of other AZ31-0.5%Sr-xY magnesium alloys.

4 Conclusions

1) The grains are further refined and the amount of β-$Mg_{17}Al_{12}$ decreases sharply in AZ31 alloy with simultaneous addition of 0.5%Sr+xY. Meanwhile, the β-$Mg_{17}Al_{12}$ phase transforms from continuous network to scattered form and the Al_2Y and Al_3Y phases are distributed both in intracrystalline and on grain boundaries.

2) The corrosion resistance of AZ31 alloy is improved apparently with simultaneous addition of 0.5%Sr+xY. With the smallest corrosion current density and corrosion rate, the corrosion resistance of AZ31-0.5%Sr-1.5%Y magnesium alloy is proved to be the best.

3) The relationship between microstructure and corrosion properties shows that the grains of AZ31 are refined with simultaneous addition of Sr and Y, and the

improvement of corrosion resistance of AZ31 lies on the content of Sr, the amount and distribution of secondary phases.

References

[1] FRIEDRICH H, SCHUMANN S. Research for a "new age of magnesium" in the automotive industry [J]. Journal of Materials Processing Technology, 2001, 117(3): 276−281.

[2] LUO A, PEKGULERYUZ M O. Review of cast magnesium alloys for elevated temperature application [J]. Journal of Materials Science, 1994, 29(20): 5259−5271.

[3] MORDIKE B L, EBERT T. Magnesium: Properties—applications—potential [J]. Materials Science and Engineering A, 2001, 302(1): 37−45.

[4] AGHION E, BRONFIN B, ELIEZER D. The role of the magnesium industry in protecting the environment [J]. Journal of Materials Processing Technology, 2001, 117(3): 381−385.

[5] YANG Z, LI J P, ZHANG J X, LORIMER G W, ROBSON J. Review on research and development of magnesium alloys [J]. Acta Metallurgica Sinica (English Letters), 2008, 21(5): 313−328.

[6] BAGHNI I M, WU Y S, LI J Q, ZHANG W. Corrosion behavior of magnesium and magnesium alloys [J]. Transactions of Nonferrous Metals Society of China, 2004, 14(1): 1−10.

[7] SUBBA RAO R V, WOLFF U, BAUNACK S, ECHKERT J, GEBERT A. Corrosion behaviour of the amorphous Mg65Y10Cu15Ag10 alloy [J]. Corrosion Science, 2003, 45(4): 817−832.

[8] YANG Ming-bo, PAN Fu-sheng, CHENG Ren-ju, TANG Ai-tao. Effect of Mg-10Sr master alloy on grain refinement of AZ31 magnesium alloy [J]. Materials Science and Engineering A, 2008, 491(1−2): 440−445.

[9] YANG Ming-bo, PAN Fu-sheng, CHENG Ren-ju, SHEN Jia. Comparison about effects of Sb, Sn and Sr on as-cast microstructure and mechanical properties of AZ61-0.7Si magnesium alloy [J]. Materials Science and Engineering A, 2008, 489(1−2): 413−418.

[10] SHANG L, JUNG I H, YUE S, VERMA R, ESSADIQI E. An investigation of formation of second phases in microalloyed AZ31 Mg alloys with Ca, Sr and Ce [J]. Journal of Alloys and Compounds, 2010, 492(1−2): 173−183.

[11] LUO T J, YANG Y S, LI Y J, DONG X G. Influence of rare earth Y on the corrosion behavior of as-cast AZ91 alloy [J]. Electrochimica Acta, 2009, 54(26): 6433−6437.

[12] TAKENAKA T, ONO T, NARAZAKI Y, NAKA Y, KAWAKAMIM. Improvement of corrosion resistance of magnesium metal by rare earth elements [J]. Electrochimica Acta, 2007, 53(1): 117−121.

[13] NIU Jie-xin, CHEN Qiu-rong, XU Nai-xin, WEI Zhong-ling. Effect of combinative addition of strontium and rare earth elements on corrosion resistance of AZ91D magnesium alloy [J]. Transactions of Nonferrous Metals Society of China of China, 2008, 18(5): 1058−1064.

[14] FAN Yu, WU Guo-hua, ZHAI Chun-quan. Influence of cerium on the microstructure，mechanical properties and corrosion resistance of magnesium alloy [J]. Materials Science and Engineering A, 2006, 433(1−2): 208−215.

[15] WEI Zhou, NAING NAING AUNG, SUN Yang-shan. Effect of antimony, bismuth and calcium addition on corrosion and electrochemical behaviour of AZ91 magnesium alloy [J]. Corrosion Science, 2009, 51(1): 403−408.

[16] ZHANG Jing-huai, NIU Xiao-dong, QIU Xin, LIU Ke, NAN Chang-ming, TANG Ding-xiang, MENG Jian. Effect of yttrium-rich misch metal on the microstructure, mechanical properties and corrosion behavior of die cast AZ91 alloy [J]. Journal of Alloys and Compounds, 2009, 471(1−2): 322−330.

Sr 和 Y 对 AZ31 镁合金组织与耐蚀性能的影响

陈 刚[1,2]，彭晓东[2,3]，范培耕[1]，谢卫东[2,3]，魏群义[2]，马 宏[2]，杨 艳[2]

1. 重庆科技学院 冶金与材料工程学院，重庆 401331；
2. 重庆大学 材料科学与工程学院，重庆 400044；
3. 国家镁合金材料工程技术研究中心，重庆 400044

摘 要：研究不同含量的 Sr 和 Y 对 AZ31 镁合金组织与耐蚀性能的影响。结果表明：添加 Sr 可以明显减小 AZ31 合金的晶粒尺寸，使 β-$Mg_{17}Al_{12}$ 相从连续网状结构转变为弥散均匀分布颗粒状，并在 AZ31-xSr 合金中生成沿晶界分布的 Al_4Sr 相。同时添加 Sr 和 Y 的晶粒细化效果好于单独添加 Sr 的。生成晶内和沿晶界分布的 Al_2Y 和 Al_3Y 相。在 AZ31 镁合金中加入 0.5%Sr+xY，其耐蚀性能明显提高。AZ31-0.5%Sr-1.5%Y 合金的腐蚀电流和腐蚀速率最小，耐蚀性能最好。

关键词：AZ31 镁合金；Sr；Y；耐蚀性能

(Edited by FANG Jing-hua)